Bulletin of the *Transilvania* University of Braşov • Vol 9(58), No. 1 - 2016
Series III: Mathematics, Informatics, Physics, 11-16

BENCHMARK SOLUTIONS FOR STOKES FLOWS IN CYLINDRICAL AND SPHERICAL GEOMETRY

Irina BLINOVA[1], Ilya MAKEEV[2] and Igor POPOV[*3]

Abstract

Benchmark analytic solutions are obtained for systems of the Stokes and continuity equations with variable viscosity and density for cylindrical and spherical geometries. These particular analytic solutions can be used for testing computational algorithms. Examples of such implementations to benchmarking of the multigrid method are presented.

2010 *Mathematics Subject Classification:* 76D07, 65N55
Key words: Stokes flow, benchmark solution.

1 Introduction

Mathematical models and computational schemes for geophysical problems are, usually, complicated [1, 2]. To be sure in the computational results, it is necessary to verify the model and the algorithm. Comparison with direct experimental result is impossible in many cases. Geophysicists, usually, compare results of different computational approaches [3, 4]. Benchmarking, i.e. comparison with known analytical result in a particular situation, is preferable. For the Cartesian geometry, a few analytical particular solutions for different situations are known (see, e.g., [5, 6, 9, 10]. As for the cylindrical and spherical geometry, the corresponding examples are rare [11, 12]. At the same time, this case is the most difficult for computing. It is interesting that the same mathematical problem appears in the theory of flows through nanostructures, e.g., nanotubes [7, 8]. In the present paper we obtain a series of analytical solutions for the Stokes and continuity equations in spherical and cylindrical geometry. For the case of varying viscosity and density, it has the form:

$$\nabla \cdot \sigma = -\rho G, \tag{1}$$

$$\nabla(\rho v) = 0. \tag{2}$$

Here$v$is velocity, $\eta$is a dynamic viscosity,$\sigma$is the total stress tensor,$p$is a pressure,$G$is a gravitational force.

[1]Department of Higher Mathematics, ITMO University, Russia, irin-a@yandex.ru
[2]Department of Higher Mathematics, ITMO University, Russia, ilya.makeev@gmail.com
[3]**Corresponding author*, Department of Higher Mathematics, ITMO University, Russia, popov1955@gmail.com

2 Problem solution in cylindrical coordinate system

We consider equations (1), (2) in cylindrical coordinates $(r, \varphi, z)$and construct a solution for the case when the functions depend only on the radius r. Let $v_r = v_r(r)$, $v_\varphi = v_\varphi(r)$, $v_z = v_z(r)$, $P = P(r)$, $\eta = \eta(r)$, $\rho = \rho(r)$, $G = G(r)$. Then, equations (1) transform to the form:

$$\begin{aligned} 2\eta r^{-1} v_r^{,} + 2\eta' v_r^{,} + 2\eta v_r^{,,} - 2\eta r^{-2} v_r - P' &= -\rho G_r, \\ \eta' v_\phi^{,} - r^{-1}\eta' v_\phi + \eta v_\phi^{,,} + r^{-1}\eta v_\phi^{,} - \eta r^{-2} v_\phi^{,} &= -\rho G_\phi, \\ \eta r^{-1} v_z^{,} + \eta' v_z^{,} + \eta v_z^{,,} &= -\rho G_z. \end{aligned}$$

Equation (2) takes the form:

$$\rho r^{-1} v_r + \rho' v_r + \rho v_r^{,} = 0$$

Integration gives us expressions for velocity component and pressure:

$$\begin{aligned} v_r &= c(r\rho)^{-1}, \\ v_\phi &= c_1 f(r) + c_2 r + C_1(r) f(r) + C_2(r) r, \\ v_z &= -\int_1^r (\eta r_2)^{-1} \left(\int_1^{r_2} r_1 \rho G_z dr_1 + c_1\right) dr_2 + c_2, \end{aligned} \tag{3}$$

and

$$P(r) = \int (\rho G_r + 2\eta r^{-1} v_r^{,} + 2\eta' v_r^{,} + 2\eta v_r^{,,} - 2\eta r^{-2} v_r) dr. \tag{4}$$

where

$$\begin{aligned} f(r) &= \exp\left(\int_1^r \left(\frac{1}{r_2} + \frac{1}{\eta r_2^3}\left(\int_1^{r_2} \frac{1}{\eta r_1^3} dr_1 + C\right)^{-1}\right) dr_2\right), \\ C_1(r) &= \int \frac{r\rho G_\phi}{\eta(f - f'r)} dr, \\ C_2(r) &= -\int \frac{f\rho G_\phi}{\eta(f - f'r)} dr \end{aligned}$$

3 Problem solution in spherical coordinate system

We seek particular solutions such that $P = P(r)$, $v_r = v_r(r)$, $v_\theta = v_\theta(r, \theta)$, $v_\phi = v_\phi(r, \theta)$, $\rho = \rho(r)$, $\eta = \eta(r)$,$G = G_r(r)$. In this case, equations (1),(2) simplify considerably. Equation (1) takes the form:

$$\frac{1}{r^2}\frac{\partial}{\partial r}\left(r^2 2\eta \frac{\partial v_r}{\partial r}\right) + \frac{1}{r\sin\theta}\frac{\partial}{\partial \theta}\left(\eta r \frac{\partial}{\partial r}\left(\frac{v_\theta}{r}\right)\sin\theta\right) -$$
$$-\frac{1}{r} 2\eta\left(\frac{1}{r}\frac{\partial v_\theta}{\partial \theta} + \frac{v_r}{r}\right) - \frac{1}{r} 2\eta\left(\frac{v_r}{r} + \frac{v_\theta}{r} cot\theta\right) - \frac{\partial P}{\partial r} = -\rho G_r,$$

$$\frac{1}{r^2}\frac{\partial}{\partial r}(r^2\eta r\frac{\partial}{\partial r}(\frac{v_\theta}{r}))+\frac{1}{r\sin\theta}\frac{\partial}{\partial\theta}(2\eta(\frac{1}{r}\frac{\partial v_\theta}{\partial\theta}+\frac{v_r}{r})\sin\theta)+$$
$$+\frac{1}{r}\eta(r\frac{\partial}{\partial r}(\frac{v_\theta}{r}))-\frac{1}{r}2\eta(\frac{v_r}{r}+\frac{v_\theta}{r}cot\theta)cot\theta-\frac{1}{r}\frac{\partial P}{\partial\theta}=0,$$
$$\frac{1}{r^2}\frac{\partial}{\partial r}(r^3\eta\frac{\partial}{\partial r}(\frac{v_\phi}{r}))+\frac{1}{r\sin\theta}\frac{\partial}{\partial\theta}(\eta(\frac{\sin\theta}{r}\frac{\partial}{\partial\theta}(\frac{v_\phi}{\sin\theta}))\sin\theta)+$$
$$+\eta\frac{\partial}{\partial r}(\frac{v_\phi}{r})+\eta(\frac{\sin\theta}{r^2}\frac{\partial}{\partial\theta}(\frac{v_\phi}{\sin\theta}))cot\theta-\frac{1}{r\sin\theta}\frac{\partial P}{\partial\phi}=0.$$

The continuity equation (2) transforms into the following one:

$$\frac{1}{r^2}\frac{\partial}{\partial r}(\rho r^2 v_r)+\frac{1}{r\sin\theta}\frac{\partial}{\partial\theta}(\rho v_\theta\sin\theta)=0.$$

For case $\eta = br^\alpha$, we obtain the following solutions of the equations:

$$v_r=\frac{1}{\rho r^2}\int\rho r v_{\theta 1}dr,\ v_\theta=v_{\theta 1}\cot\theta,\ v_\phi=r(c_1\int\frac{1}{\eta r^4}dr+c_2)\sin\theta, \qquad (5)$$

$$P(r)=\int(\rho G_r+\frac{1}{r^2}\frac{\partial}{\partial r}(r^2 2\eta\frac{\partial v_r}{\partial r})-\eta\frac{\partial}{\partial r}(\frac{v_{\theta 1}}{r})-4\eta\frac{v_r}{r^2}+2\eta\frac{1}{r^2}v_{\theta 1})dr. \qquad (6)$$

Here b,α are constants,$v_{\theta 1}=Ar^{C_1}+r^{C_2}$, $C_{1,2}=\frac{1}{2}(-(\alpha+1)\pm\sqrt{(\alpha+1)^2+4\alpha})$, $\alpha\leq -3-2\sqrt{2}$ or $\alpha\geq -3+2\sqrt{2}$.

4 Multigrid method and numerical convergence tests

The scheme for solving the Stokes equations by multigrid method in Cartesian coordinates is described in book [1]. We derive similar schemes for cylindrical and spherical geometries.As usual, an algorithm of multigrid method contains smoothing, restriction and prolongation operations. Cylindrical coordinates are orthogonal coordinates. So, the implementation of the prolongation and restriction operations in our method is not different from that in the case of Cartesian coordinates. Smoothing operation can be implemented on the basis of the Gauss-Seidel iterations with pressure updates computed from local divergence scaled to local viscosity.

This scheme for cylindrical coordinates has been tested by comparing with the analytical solutions of (1), (2). The scheme of algorithm testing is as follows. Consider some particular analytical solution (3), (4):$v_r = r^{-1}$,$v_\phi = r + r^{-2}$,$v_z = r^{-1}$,$P(r) = 2r^{-1}$in the domain $1 \leq r \leq 2$,$0 \leq \phi \leq 1$,$0 \leq z \leq 1$ ($\rho = const$,$G = 0$,$\eta = ar$). We calculate the values for velocity and pressure given by our analytical solution and take these values as the boundary conditions for numerical algorithm. The deviation of the numerical solution values from the analytical solution is related with the error of the multigrid scheme. The dependence of the relative errorε on the grid step$d$ (in logarithmic scale) for multigrid scheme is shown in Figure.1. Positive slope means the convergence of the algorithm.

In the same way, we test the scheme for spherical geometry. Consider a ?ow in a parallelepiped (in spherical coordinates): $1 \leq r \leq 2$,$0.5 \leq \theta \leq 1.5$,$0 \leq \phi \leq 1$.

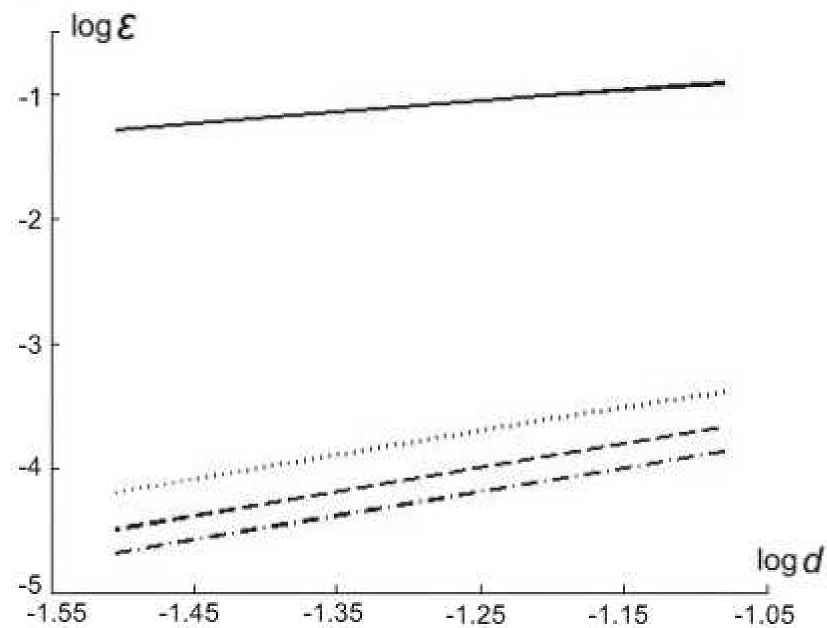

Figure 1: Error norm via the grid resolution in logarithmic scale for L_2-error: solid line- pressure, dashed line- v_r , dotted line- v_ϕ , dash-dot line- v_z.

We take $G_r = 10$,$G_\theta = 0$,$G_\phi = 0$,$\rho = const(\rho = 5)$, $\eta = cr^3(c = 1)$. Benchmark solution (6) has the following form:

$$v_r = r^{\sqrt{7}-2}/\sqrt{7},\ \ v_\theta = r^{\sqrt{7}-2}\cot(\theta),\ \ v_\phi = r^{-5}\sin(\theta),\ \ P(r) = 1.176r^{\sqrt{7}} + \rho G_r r.$$

Correspondingly, the error norms convergence is characterized by the following picture (Figure.2) showing the relative errorε dependence on the grid step$d$ (in logarithmic scale).

5 Acknowledgements

The authors thanks Prof. T. Gerya and Prof. P. Tackley for interesting discussions. This work was partially financially supported by the Government of the Russian Federation (grant 074-U01), by Ministry of Science and Education of the Russian Federation (GOSZADANIE 2014/190, Projects No 14.Z50.31.0031 and No. 1.754.2014/K), by grant MK-5001.2015.1 of the President of the Russian Federation and by grant 16-11-10330 of Russian Science Foundation.

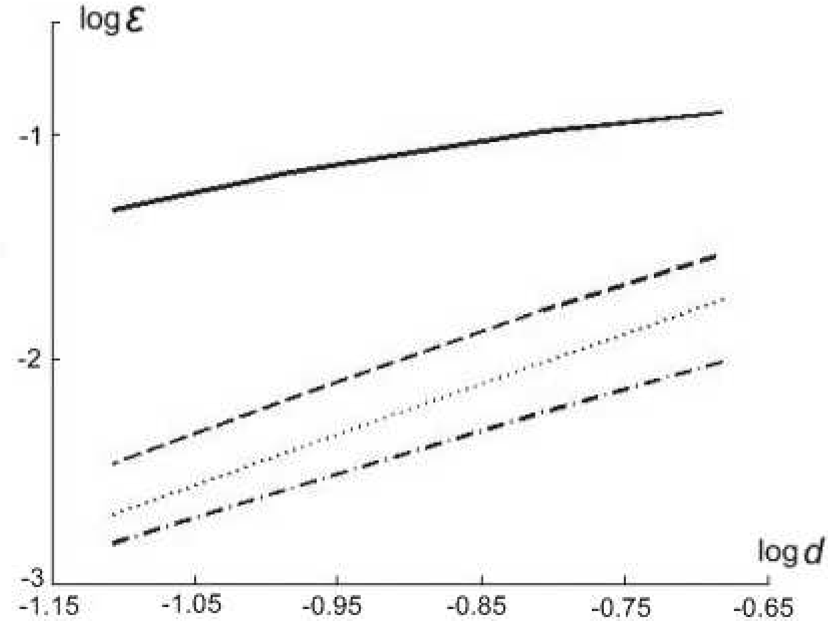

Figure 2: Error norm via the grid resolution in logarithmic scale for L_2-error: solid line–pressure, dashed line $-v_r$, dotted line $-v_\theta$, dash-dot line $-v_\phi$.

References

[1] Gerya, T., *Introduction to numerical geodynamic modelling*, Cambridge University Press, Cambridge, 2010.

[2] Ismail-Zadeh, A. and Tackley, P., *Computational methods for geodynamics*, Cambridge University Press, Cambridge, 2010.

[3] Deubelbeiss, Y. and Kaus, B. J., *Comparison of Eulerian and Lagrangian numerical techniques for the Stokes equations in the presense of strongly varying viscisity*, Physics of Earth and Planetary Interior. **171** (2008), 92-111.

[4] Duretz,T., May, D.A., Gerya, T. V. and Tackley, P. J., *Discretization errors and free surface stabilization in the finite-difference and marker-in-cell method for applied geodynamics: a numerical study*, Geochemistry, Geophysics, Geosystems. **12** (2008), Q07004.

[5] Blankenbach B., Busse, F., Christensen, U., Cserepes, L., Gunkel, D. and Hansen, U., *A benchmark comparison for mantle convection code*, Geophysical Journal International. **98** (1989), 23 - 38.

[6] Busse, F., Christensen, U., Clever, R., Cserepes, L., Gable, C. and Giannandrea, E., *3-D convection at infinite Prandtle number in Cartesian geometry*

- *a benchmark comparison*, Geophysical and Astrophysical Fluid Dynamics. **75** (1994), 39 -59.

[7] Popov, A. I., Gerya, T. V., Lobanov, I. S. and Popov, I.Yu. *Benchmark solutions for nanoflows*, Nanosystems: Physics, Chemistry, Mathematics, **5** (2014), 391 -399.

[8] Popov, A. I., Gerya, T. V., Lobanov, I. S. and Popov, I. Yu. *On the Stokes flow computation algorithm based on Woodbury formula*, Nanosystems: Physics, Chemistry, Mathematics, **6** (2015), 140 -145.

[9] Popov, I. Yu., Lobanov, I. S., Popov, S. I., Popov, A. I. and Gerya, T. V. *Practical analytical solutions for benchmarking of 2-D and 3-D geodynamic Stokes problems with variable viscosity.* Solid Earth. **5** (2014), 461 - 476.

[10] Tosl, N., Stein, C., Noack, L., Huttig, C., Maierova, P., Samuel, H., Davies, D. R., Wilson, C. R., Kramer, S. C., Thieulot, C., Glerum, A., Fraters, M., Spakman, W., Rozel, A. and Tackley, P. J. *A* community benchmark for viscoplastic thermal convection in a 2-D square box. Geochemistry, Geophysics, Geosystems, (2015). DOI 10.1002/2015GC005807.

[11] Tackley, P. J. *Modelling compressible mantle convection with large viscosity contrasts in a three-dimensional spherical shell using the yin-yang grid.* Physics of Earth and Planetary Interior, **171** (2008), 7 - 18.

[12] van Keken, P. E., Currie, C., King, S. D., Behn, M. D., Cangleoncle, A., He, J., Katz, R. F., Lin, S. C., Parmentier, E. M., Spiegelman, M. and Wang, K. *A community benchmark for subduction zone modeling*, Physics of Earth and Planetary Interior, **171** (2008), 187 -197.